Interannual variability in lower trophic levels on the Alaskan Shelf

Sonia D. Batten[a],[*], Dionysios E. Raitsos[b], Seth Danielson[c], Russell Hopcroft[c], Kenneth Coyle[c], Abigail McQuatters-Gollop[d]

[a] Sir Alister Hardy Foundation for Ocean Science, c/o 4737 Vista View Cr, Nanaimo, BC, Canada V9V 1N8
[b] Plymouth Marine Laboratory, Prospect Place, The Hoe, Plymouth PL1 3DH, United Kingdom
[c] Institute of Marine Science, University of Alaska Fairbanks, 120 O'Neill, P.O. Box 757220, Fairbanks, AK 99775-7220, USA
[d] Centre for Marine and Conservation Policy, Plymouth University, Drake Circus, Plymouth PL4 8AA, United Kingdom

ARTICLE INFO

ABSTRACT

This study describes results from the first 16 years of the Continuous Plankton Recorder (CPR) program that has sampled the lower trophic levels (restricted to larger, hard-shelled phytoplankton and robust zooplankton taxa) on the Alaskan shelf. Sampling took place along transects from the open ocean across the shelf (to the entrance to Prince William Sound from 2000 to 2003 and into Cook Inlet from 2004 to 2015) to provide plankton abundance data, spring through autumn of each year. We document interannual variability in concentration and composition of the plankton community of the region over this time period. At least in part and through correlative relationships, this can be attributed to changes in the physical environment, particularly direct and indirect effects of temperature. For example; spring mixed layer depth is shown to influence the timing of the spring diatom peak and warmer years are biased towards smaller copepod species. A significant positive relationship between temperature, diatom abundance and zooplankton biomass existed from 2000 to 2013 but was not present in the warm years of 2014 and 2015. These results suggest that anomalous warming events, such as the "heat wave" of 2014–2015, could fundamentally influence typical lower trophic level patterns, possibly altering trophic interactions.

1. Introduction

The south Alaskan Shelf region that encompasses the large inlets of Cook Inlet (CI) and Prince William Sound (PWS) and the outer shelf of the northern Gulf of Alaska is a productive, dynamic, subarctic shelf system supporting numerous valued marine resources such as commercially-harvestable fish (e.g. herring, salmon, groundfish), large marine mammals (e.g. belugas, humpback whales), and seabirds. Lower trophic level productivity underpins this ecosystem but our understanding of plankton variability in this region is still somewhat limited.

It is recognized now that forcing of marine ecosystems occurs at multiple temporal and spatial scales. It is challenging to attempt to understand the impacts of climate change on marine organisms and detect trends in data when there is high interannual variability in both the physical forcing and biological responses. For example, restoration projects for injured resources following the Exxon Valdez oil spill in PWS in 1989 have struggled with teasing apart the impacts of this one-off catastrophic event from naturally-induced variability (EVOS Trustee Council, 2010). Natural, rather than human-related, processes known to influence this region are numerous. For example, on seasonal and interannual time scales the strength of the Alaskan shelf and Alaskan Coastal currents are mediated by freshwater run-off and winds (Royer, 1979; Stabeno et al., 2004; Weingartner et al., 2005), persistent coastal downwelling in contrast to most eastern Pacific boundary regions, and eddy-mediated cross-shelf transport of organisms and nutrients (Okkonen et al., 2003; Ladd et al., 2005). More quasi-decadal time scale influences are the change in sign of the Pacific Decadal Oscillation (PDO), which is based on the analysis of Mantua et al. (1997) and is the first mode of ocean surface temperature variability in the North Pacific Ocean. Historically it has been a good indicator of weather patterns that persist for a decade or more but has more recently been switching state approximately every 5 years. Positive (negative) PDO values are associated with warmer (cooler) than normal conditions in the NE Pacific. A second medium time-scale influence is the North Pacific Gyre Oscillation (NPGO), a climate pattern that emerges as the second dominant mode of sea surface height variability in the Northeast Pacific Ocean (Di Lorenzo et al., 2008, http://www.o3d.org/npgo/). When the NPGO index is positive the westerly winds over the eastern North Pacific are often stronger than normal, influencing the circulation processes. Moderate to strong El Niño and La Niña events are also evident on the

---

Alaskan Shelf (Weingartner et al., 2002). Regime shifts, which may be triggered by the climate processes described above, have periodically occurred with lower frequency, such as the 1976 shift which changed Alaskan fisheries from shrimp to fish dominated (Francis and Hare, 1994). More recently, anomalous warming across a wide expanse of the Northeast Pacific occurred late in 2013 and persisted through 2014 (Bond et al., 2015). Nicknamed "the Blob" and succeeded by a strong El Nino in 2015, the Alaskan shelf has been influenced by these strong warming events for at least two consecutive years (DiLorenzo and Mantua, 2016).

With short generation times, limited mobility and lack of a commercial harvest, plankton often respond to changes in their environment more rapidly and less ambiguously than higher trophic levels, so that a relatively short time series of plankton information can provide insights into the responses of the shelf ecosystem to some of the processes described above. Primary productivity is strongly seasonal in this region, owing primarily to the relatively high latitude and low light levels in winter. Mueter et al. (2009) report that although there are clear peaks in satellite-derived chlorophyll-*a* levels in spring and autumn (owing to the spring bloom and replenishment of nutrients by autumn storms respectively) there is in fact a single broad peak of productivity in the Gulf of Alaska through summer that is heavily grazed by zooplankton and so results in low phytoplankton standing stocks in summer. There has been significant interannual variability in chlorophyll-*a* concentrations over the previous decade and more, with positive anomalies in years with reduced cloud cover, lower SST and reduced downwelling-favourable winds (Waite and Mueter, 2013). These observations do not necessarily represent variability in primary productivity but may suggest that strong cyclonic circulation does not favour high chlorophyll-*a* concentrations throughout the Gulf of Alaska.

Previous studies of zooplankton on the shelf (Coyle and Pinchuk, 2003) and in PWS (Cooney et al., 2001) suggest a strong seasonal community dominated by copepods (with significant contributions from other taxa such as cnidarians on the shelf, euphausiids, pteropods and larvaceans seasonally in PWS). While small-medium sized copepod species dominated in terms of abundance at all times of year, the biomass in spring and early summer was dominated by larger copepods that spend the winter in diapause at depth. Negative salinity anomalies, followed by temperature, were the strongest influencers of the zooplankton community (Coyle and Pinchuk, 2003).

The Continuous Plankton Recorder (CPR) was designed to be towed behind commercial ships and to sample plankton from near surface waters over large spatial scales (Batten et al., 2003a). This study describes results from the first 16 years of the Continuous Plankton Recorder (CPR) program that has sampled the lower trophic levels of the south-central Alaska Shelf, on a seasonal basis from spring to autumn. Although restricted to larger, hard-shelled phytoplankton and robust zooplankton taxa, this dataset is complementary to previous studies which have been more geographically focussed but with reduced temporal coverage. The CPR data are now sufficient to examine the interannual variability of the plankton populations with respect to changing oceanographic conditions of the region.

2. Methods

2.1. Sampling

The CPR was towed behind a volunteer commercial vessel making the sampling cost-effective, but with limited ability to control the timing of the sampling and no ability to determine the transect position. The original transect operated from 2000 between ports in California, USA and PWS, with sampling normally stopping at Hinchinbrook Entrance. Owing to changes in shipping activities the transect was changed in 2004 to a route from the mouth of Juan de Fuca Strait (at the border of British Columbia, Canada, and Washington State, USA) to Anchorage, with sampling normally stopping in CI between about 59-
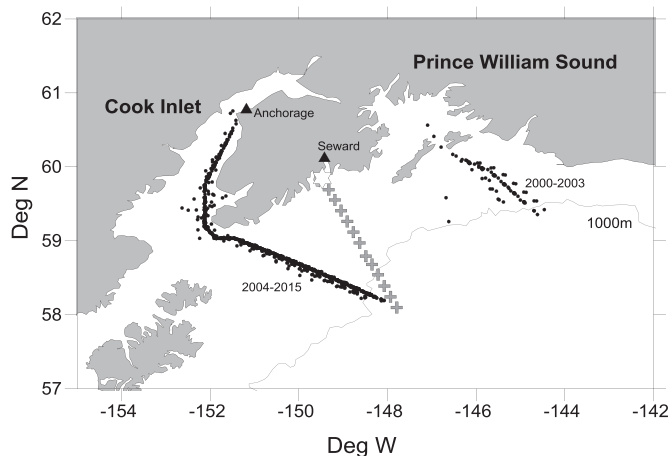

Fig. 1. Location of CPR samples and years when each transect was sampled (see Table 1 for data availability in each year). The midpoint of each 18.5 km CPR sample used in this study is shown as a dot. Note the consistency of the Cook Inlet transect; there are over 50 separate monthly transects but they overlap almost entirely. Two other data sources used in the study are shown; Seward Line sampling stations are shown as " + " and the GAK1 station as a star.

60°N (Fig. 1). Start and end of sampling was always at the discretion of the vessel's Captain. The second transect was remarkably consistent with almost identical transect positions each month, particularly at the northern end with which this study is concerned. Frequency of sampling was at approximately monthly intervals in most years (occasionally two transects occurred in one calendar month), commencing in about April and ending in about September, but occasionally sampling March and October (Table 1). Mechanical failures, human error and marine debris mean that in any one year, one or two months may have reduced, or no, data available. In summary, while the available data have gaps, they represent a sufficiently lengthy and spatially expansive time series of seasonal data with which to examine lower trophic level variability in this region.

A summary is given here but for a full description of the CPR instrument and sampling protocols see Batten et al. (2003a) and see Richardson et al. (2006) for data analysis methods.

The CPR was towed in the wake of the ship at a depth of about 7 m. Water and plankton enter the front of the CPR through a small square aperture (sides of 1.27 cm), pass along a tunnel, and then through the silk filtering mesh (with a mesh size of 270 μm) which retains the plankton and allows the water to exit at the back of the machine. The movement of the CPR through the water turns an external propeller which, via a drive shaft and gear-box, moves the filtering mesh across the tunnel at a rate of approximately 10 cm per 18.5 km of tow. As the

Table 1
Months for which data were available in each year.

Transect	Year	Mar	Apr	May	Jun	Jul	Aug	Sep	Oct
PWS	2000	X	X			X	X		
PWS	2001		X	X	X			X	
PWS	2002		X			X			X
PWS	2003			X			X		
Cook Inlet	2004	X	X		X	X	X		
Cook Inlet	2005		X	X		X	X		
Cook Inlet	2006	X	X			X	X	X	X
Cook Inlet	2007		X		X		X	X	
Cook Inlet	2008				X			X	
Cook Inlet	2009		X	X	X		X		
Cook Inlet	2010		X			X		X	
Cook Inlet	2011		X	X		X	X	X	
Cook Inlet	2012		X	X	X	X		X	X
Cook Inlet	2013		X	X	X	X	X	X	
Cook Inlet	2014	X	X	X	X	X	X		
Cook Inlet	2015		X		X		X	X	

filtering mesh leaves the tunnel it is covered by a second band of mesh so that the plankton are sandwiched between these two layers. This mesh and plankton sandwich is then wound into a storage chamber containing buffered 40% formaldehyde preservative (which dilutes in the seawater to a concentration of about 4%, sufficient to fix and preserve the plankton). After each transect the CPR was transferred to a laboratory, where the samples were unloaded. The towed mesh was processed according to standard CPR protocols; first cut into separate samples (each representing 18.5 km of tow and about 3 m^3 of seawater filtered) which were randomly apportioned amongst the analysts for plankton identification and counting. Every fourth oceanic sample was distributed for analysis with the remainder being archived, but over the Alaskan shelf consecutive samples were processed. The ship's log was used to determine the mid-point latitude and longitude of each sample (shown in Fig. 1), along with the date and time.

2.2. Taxonomic analysis

As with all plankton samplers the CPR has biases. The mesh size is 270 μm and so organisms with dimensions smaller than this may not be quantitatively sampled, however, the effective mesh size may be much smaller depending on the abundance and morphology of plankton that are caught (see Batten et al., 2003a for more details) and organisms such as coccolithophores with a diameter of a few tens of microns are caught and identified. The formaldehyde preservative used in the instrument does not fix naked dinoflagellates or ciliates so these groups are not at all represented in the database. The sampling method can also result in damage to the organisms so fragile groups, especially gelatinous plankton, may only be identifiable to a coarse level.

There were four steps in analysing the plankton retained in a CPR sample. The first step was the assessment of phytoplankton colour (the greenness of the sample, or Phytoplankton Colour Index, PCI), which was determined by comparison with standard colour charts. This is a semi-quantitative representation of the total phytoplankton biomass and includes the organisms that are too fragile to survive the sampling process intact but which leave a stain on the mesh (Batten et al., 2003b; Raitsos et al., 2013). Hard-shelled phytoplankton were then semi-quantitatively counted under a purpose-built microscope by viewing 20 fields of view (diameter 295 μm) across each sample under high magnification (× 450) and recording the presence of all the taxa in each field (presence in 20 fields is assumed to reflect a more abundant organism than presence in 2 fields for example). Small zooplankton were then identified and counted from a sub-sample by tracking across the filtering mesh with the microscope objective (a 2 mm diameter field of view = 2% of the sample width) whilst all zooplankton larger than about 2 mm were removed from the mesh and counted, usually without sub-sampling. Identification in all cases was carried out to the most detailed practicable taxonomic level and was a compromise between speed of analysis and scientific interest. For example, since copepods make up the majority of the zooplankton and remain mostly intact after sampling, most copepods were identified to species level whilst rarer groups, or those not preserved well by the sampling mechanism (such as chaetognaths), were identified to a lower level such as phylum. A list of taxa and their abundance in each sample was thus generated, and from this summary indices (such as estimated zooplankton biomass, total diatom abundance, etc.) were also calculated.

2.3. Comparison of CPR Phytoplankton indices and satellite data

To compare the in situ phytoplankton seasonal cycles (PCI and diatoms from the CPR data) with a satellite-derived ocean colour dataset, the monthly near-surface Chlorophyll-*a* (Chl-*a*) was acquired from NASA's Oceancolor website (http://oceancolor.gsfc.nasa.gov). The Moderate-resolution Imaging Spectroradiometer (MODIS on-board the Aqua platform) 4 km resolution Chl-*a* data were processed for the period 2003–2011 (O'Reilly et al., 2000). Standard NASA algorithms

were used for Chl-*a* (OC3) estimates; these are routinely processed by the Ocean Biology Processing Group at the Goddard Space Flight Centre (Feldman and McClain, 2012). Using the monthly mean datasets, we constructed the area-averaged monthly climatologies.

Remotely sensed Chl-*a* data have known limitations especially in coastal, optically complex, Case II waters where suspended sediments, particulate matter and/or dissolved organic matter do not covary in a predictable manner with Chl-*a* (IOCCG, 2000). For example, scattering by sediments in turbid waters and underwater reflectance from shallow shelf regions may result in relatively high water-leaving radiance in the near-infrared (NIR) wavelengths, which could overestimate the correction term. For this reason satellite data from CI were excluded. Even so, the Chl-*a* data used in the analysis may be influenced (generally resulting in an overestimation) by the factors mentioned above, especially in the most coastal waters and/or very shallow waters of the Alaskan Shelf area. However, the scope of the current study is to compare the general variability of satellite-derived Chl-*a* and CPR phytoplankton in the Alaskan Shelf, regardless of absolute concentrations. In addition, to gain confidence on the variability and pattern of satellite derived Chl-*a*, we also compared the MODIS results with those from SeaWiFS. The area-averaged monthly means, and the seasonal climatologies of the two satellite-derived Chl-*a* datasets were significantly correlated ($r^2 = 0.78$, $p < 0.0001$, and $r^2 = 0.98$, $p < 0.0001$ respectively).

2.4. Analysis of CPR plankton time series

All shelf samples were extracted from the database. These samples were south of PWS 2000–2003, and in CI and southeast of it 2004–2015 owing to the change in transect position.

2.4.1. Abundance and seasonal timing

The mean abundance per sampling event (monthly transects) was calculated for the entire shelf region for various taxonomic groupings (e.g., total mesozooplankton, large copepod abundance, large diatom abundance, dinoflagellates, etc). Mean seasonal cycles were calculated by averaging the monthly averages for each month of the year (restricted to March to October). Seasonal timing and annual abundance indices were calculated using a method proposed by Grieve et al. (2005) that relies on cumulative integration. In this case we integrated between day 60 and day 300 each year (assuming 0 abundance on days 60 and 300), and summed daily values to give a cumulative total for the year. All years had 5–6 samplings, spaced at least monthly, except 2003, 2008 and 2010 so these years should be treated with caution if data are shown. The day of the year when 50% of the cumulative abundance occurred was calculated (this is the mid-season, as an index of timing). An annual abundance anomaly (Log10, based on the geometric mean of all years) was calculated for each year for the cumulative integrated biomass/abundance at day 300.

2.4.2. Community composition

The same samples as described above were used but individual taxon abundances were extracted to examine interannual variability in the taxa present. Data were divided into spring (April, May and June) and late summer/autumn (August and September). Phytoplankton and mesozooplankton were treated separately (microzooplankton were excluded). The mean annual abundance of each taxon in each group (phyto or zooplankton, spring or autumn) was calculated and then the data were transformed (Log{x + 1}) to reduce the impact of dominant taxa. Bray Curtis dissimilarities were calculated for each pair of years, and then NMDS (in the SYSTAT software package) used to display the ordinations in 2 dimensions.

2.4.3. Copepod community length

Size of its members is an important zooplankton community attribute, likely governing trophic interactions. Change in size can only be

accurately determined for the copepods captured by the CPR as they are the only important and dominant group identified mostly to species. The methodology of Richardson et al. (2006) was applied to the copepod counts. Mean copepod community size ($\overline{S}$) for each sample was calculated:

$$\overline{S} = \frac{\sum_{i=1}^{N} (L_i . X_i)}{\sum_{i=1}^{N} X_i}$$

Where L is the mid-range adult female total length (mm) per species (i) obtained from Chihara and Murano (1997) and when not available, from Razouls et al. (2012), and X is its abundance.

Monthly means were calculated for the five warmest (2001, 2003, 2005, 2014 and 2015) and five coldest years (2002, 2007, 2008, 2009 and 2012), based on the GAK1 dataset.

2.4.4. Physical data

In order to explain the patterns within the plankton data, time series of physical variables were used. Temperature observations were available from the GAK1 dataset (location shown on Fig. 1), available at http://www.ims.uaf.edu/gak1/, which was the geographically closest source to the CPR data of seasonally resolved in situ temperature. Monthly measurements have been made at GAK 1 from 1970 to present from surface to depth. For this study, a mean of the four upper-most water column measurements was calculated (0, 10, 20, and 30 m) from each month to represent water temperatures that most of the planktonic organisms would have experienced. Where a month was not sampled in a particular year, the long term mean for that month was used instead to create an unbroken time series of March to October values.

Some in situ temperature measurements were also available from a logger on the CPR itself from 2000 to 2002 and 2011–2015. For each transect where a logger was fitted, temperature was recorded every 5 min (15 min in 2000 to 2002) for the duration of the tow. Data collected between 59°N and 60°N (2000–2002) or 57.5°N to 59°N (2011 onwards) were averaged to represent temperature on the shelf at the depth of the CPR each sampled month.

The CPR transect into Cook Inlet intersects with the outermost stations of the Seward Line (Fig. 1). The mixed layer depth (MLD), an index of stratification (Potential Energy) and salinity measurements were available from the Seward Line cruises in May of each year to provide spring water column characteristics (the Seward Line is only sampled in May and September/October so May was selected as best describing the conditions which might influence the plankton through spring and summer when most of the CPR sampling occurred). A CTD was deployed at each station and the MLD computed as the depth at which the density is greater than 0.03 kg m^{-3} at 5 m depth. The stratification parameter, the potential energy required to redistribute the water-column mass by complete vertical mixing (J/m^3), was also computed (Simpson et al., 1977). The thermocline is not necessarily fully established by the time of the May cruise leading to variability along the line. We therefore averaged the values for all stations to provide the best index of spring water column stability. Salinity data (from all depths) were also available from all stations along the Seward Line.

3. Results

3.1. The physical environment

Physical data (SST, salinity, Potential Energy and Mixed Layer Depth) are shown in Fig. 2. The early part of the time series was relatively cool and then temperatures increased from 2003 to 2005. Another cool period followed, with 2008 being the coldest year of the record, before temperatures rose in 2014 as the influence of the anomalous off-shore warming became apparent. The time series ends with warm conditions resulting from the 2014 anomaly and the 2015 El

Niño. Salinities on the Seward Line stations in May each year were freshest in 2004 and 2015 (warm years, so likely some influence of early, or increased, snow melt) and most saline in 2000 and 2013 but note that outer stations were not sampled in 2008 (the coldest year). Water column stability indices show that in the earlier warm period of 2004–05 the MLD was shallow and the energy required to mix the water column was large (high Potential Energy), indicating stronger stratification. While the colder period was missing data from 2008, 2007 showed a deeper MLD and lower Potential Energy, suggesting weaker stratification. In the more recent warm period of 2014 and 2015 the MLD was shallow in 2014 but deeper in 2015 and the Potential Energy was quite low in both years, suggesting quite weak stratification.

3.2. Abundance and seasonal timing

3.2.1. Phytoplankton

The phytoplankton counts from the CPR are not representative of the whole phytoplankton community, with a large mesh compared to most of the cells, and a preservative unsuitable for athecate cells; however, it is an internally consistent time series and larger and more robust phytoplankton are captured well. A comparison with satellite-derived chlorophyll-a data demonstrates that CPR phytoplankton data generate realistic seasonal cycles (Fig. 3). The CPR PCI values peak on average one month earlier than the satellite measurements of chlorophyll-a in both the spring and autumn peaks, but the diatom abundances match the satellite-derived seasonal cycle very closely. The general pattern shows two diatom blooms; in spring and a lesser peak in late summer/autumn. This is typical of a shelf system where autumnal storms may increase mixing, bringing up nutrients and allowing a second phytoplankton bloom while light levels are sufficient. Thecate dinoflagellates are most abundant only in the summer and autumn when waters are warmer. The PCI index closely follows the diatom cycle, but increases earlier (as evident in Fig. 3 when compared with the satellite chlorophyll data). The difference between spring and autumn PCI is less than the difference between spring and autumn diatoms, perhaps because the index also incorporates a signal from the dinoflagellates.

Annual abundance anomalies of diatoms (calculated as previously described for March to October) are shown in Fig. 4. During the first 14 years of the time series it was noted that there was a moderate, positive, significant correlation between diatom abundance and temperature (r^2 = 0.28, p < 0.05 with either the annual mean GAK 1 temperature, or with the annual PDO index) with warm, PDO positive years having greater numbers of diatoms (Fig. 4). However, 2014 and 2015 did not follow this pattern and abundances were low, despite the very warm conditions. Numbers were also low in 2011 which was neither a warm nor cold year.

Thecate dinoflagellates are numerically much less dominant than diatoms in CPR samples, ranging from between one third and one sixtieth of the diatom abundance. There were no significant relationships between the dinoflagellate mean annual abundance anomalies and physical variables, however, the linear decline through time is significant (r^2 = 0.23, p < 0.05). This could be because of a regional difference as the region south of PWS, sampled only in 2000–2003, had consistently higher abundances of dinoflagellates than the Cook Inlet and nearby shelf region sampled from 2004 and afterwards, however, since the two regions were not sampled simultaneously we cannot be certain. From 2004 onwards the pattern shows inter-annual variability with no trend.

Although the CPR sampling resolution is not sufficient to identify the exact timing of the spring phytoplankton bloom, we focused on just the spring diatom data, integrating abundances between days 60 and 180 (as described previously for the whole season) and taking the day of the year where 75% of the spring diatom abundance was reached as an index of spring timing (years 2002, 2003, 2008 and 2010 were not
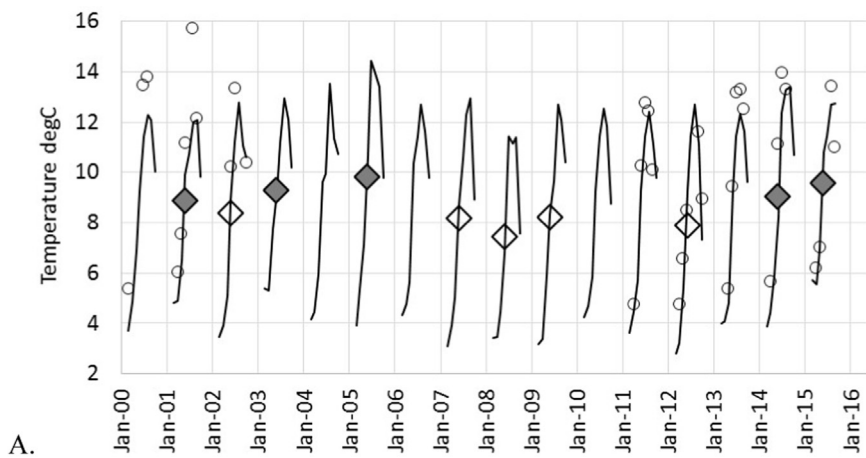
Fig. 2. Physical variables. Panel A. Mean monthly (Mar-Oct) SST from the GAK1 station (lines) and mean monthly in situ SST from loggers on the CPR (○). Filled diamonds indicate the mean annual (March-October) temperature for the 5 warmest years, unfilled diamonds indicate the mean for the 5 coldest years. Panel B. Salinity Data from May cruises on the Seward Line (error bars show st. dev.) Panel C. Water column stability shown by: solid line – mean Mixed Layer Depth, dashed line – mean Potential Energy.
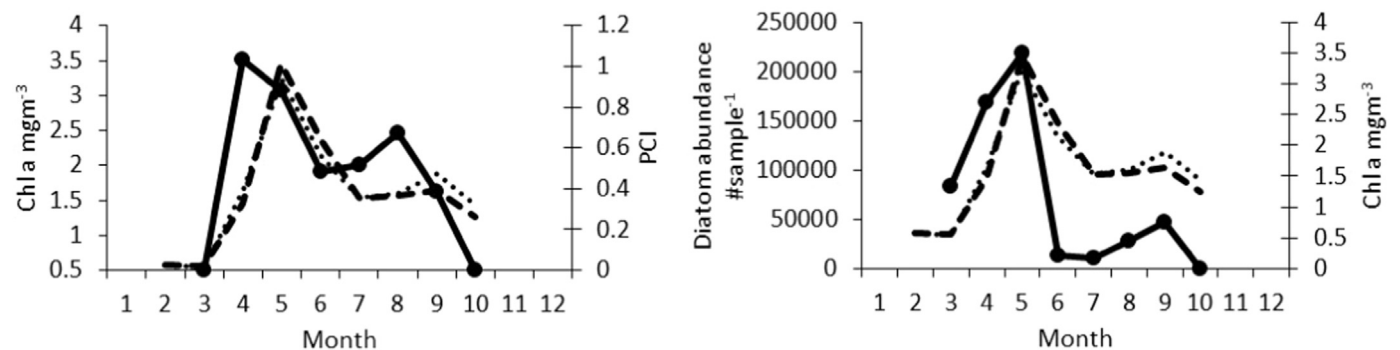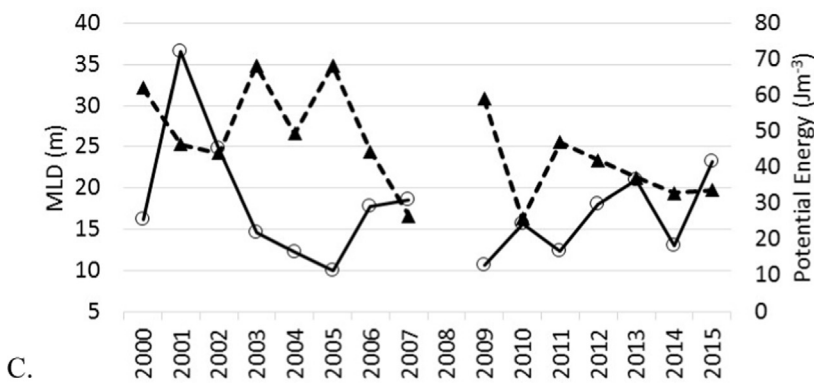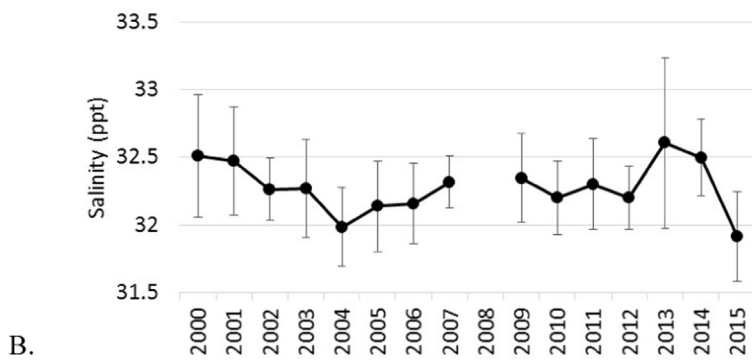
Fig. 3. Mean monthly phytoplankton indices from CPR data (solid line, Phytoplankton Colour Index at left, diatom abundance at right) and satellite-derived chlorophyll-a (from MODIS, heavy dashed line and SeaWiFS, lighter dashed line on both graphs) for the region shown in Fig. 1, excluding Cook Inlet.
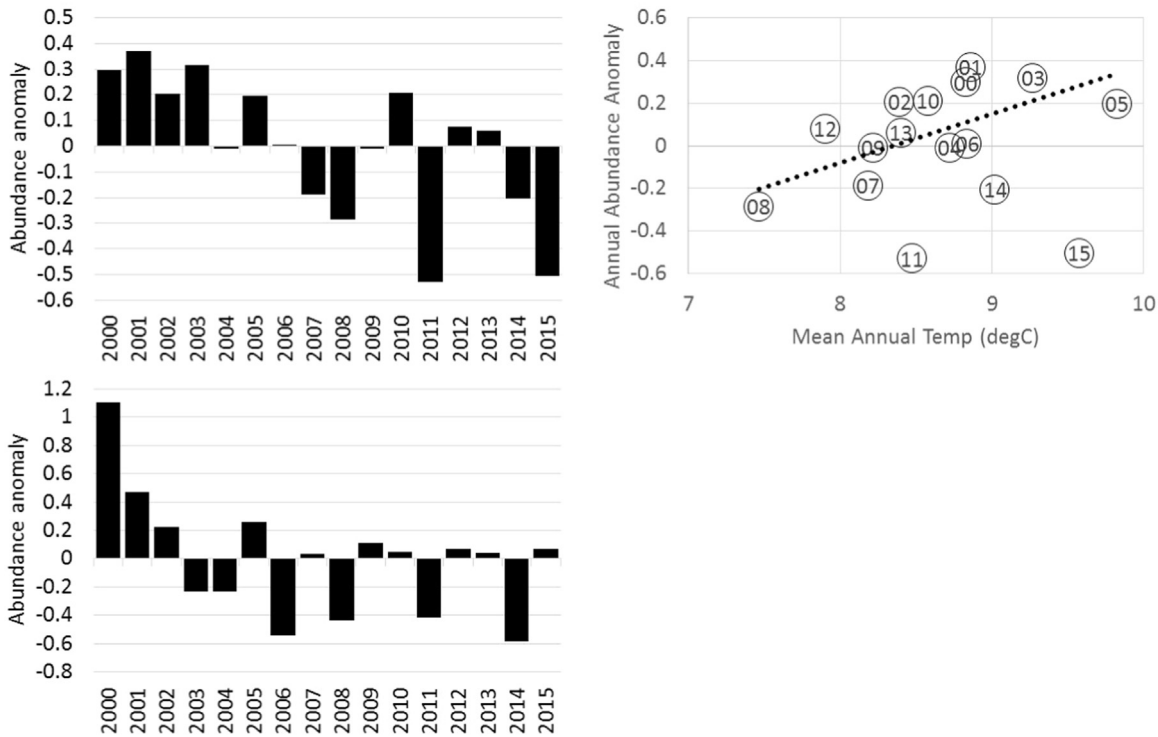
Fig. 4. Annual abundance anomalies of diatoms (top left) and thecate dinoflagellates (bottom left). Right panel shows the relationship between diatom abundance and mean temperature (mean of March to October monthly GAK1 temperature). The dashed line indicates the relationship from 2000 to 2013 with year shown inside each data point.
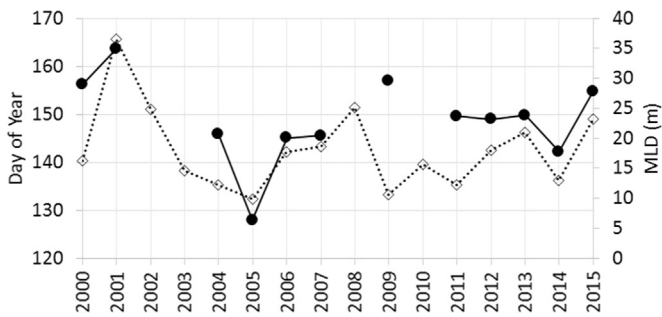

Fig. 5. Spring diatom timing (day of year when 75% of the integrated daily abundance at day 180 was reached) for years when sampling resolution was sufficient (solid line), together with the time-series of mean May MLD along the Seward Line (dashed line).

sampled sufficiently often in the spring to calculate this index). There was no significant correlation between spring timing and temperature as indexed by mean annual GAK 1 temperature or the PDO (although 2005 and 2014 did have the earliest dates and the modest relationship was negative), however, the Seward Line MLD correlated significantly with diatom timing (n = 11, r^2 = 0.39, p < 0.02), so that in years with a greater MLD in May the spring peak was later (Fig. 5). The correlation with potential energy of the water column was negative, but non-significant. There was also a significant correlation between diatom spring timing and the NPGO (p < 0.02) so that with a positive NPGO (stronger westerly winds are associated with positive NPGO further south and through the shelf edge currents influence MLD in this region), the diatom peak is later.

3.2.2. Zooplankton

Estimated mesozooplankton biomass is a summary index of the overall zooplankton community, and the anomaly time series is shown in Fig. 6, together with annual abundance anomalies of five of the dominant taxonomic groups (large copepods > 2 mm length, small copepods < 2 mm length, euphausiids, hyperiids, and pteropods). Also shown is an index of seasonal timing for each zooplankton variable, as

day of the year when 50% of the integrated daily biomass/abundance was reached. No long term trends are evident in the time series, with the exception of hyperiid abundance which has generally increased over the 15 year period. Between-year variability is large in all six cases.

There was a very strong positive correlation between the annual diatom abundance and zooplankton biomass anomalies from 2000 to 2013 (r^2 = 0.49, p < 0.005) so that years with a higher abundance of diatoms had a higher zooplankton biomass, suggesting a trophic link. This relationship was not present in 2014 and 2015 which had high zooplankton biomass but low diatom abundance. All of the five major zooplankton taxonomic groups had positive correlations between their abundance and diatom abundance until 2013, but none were individually significant. Similarly, there were positive correlations between most of the zooplankton groups and temperature, however, none were significant at the p < 0.05 level. Temperature does, however, have an effect on seasonal timing. The mid-point of the zooplankton biomass season is later in cold years. This is also true for small and large copepods. For small copepods this is a strong, negative relationship between seasonal timing and the PDO/temperature (r^2 = 0.5, p = 0.003 with the PDO), but less so for large copepods (r^2 = 0.2, p = 0.09) and for both groups the difference in timing between the earliest and latest years was more than two months. There were no significant relationships between euphausiids, hyperiids and pteropod seasonal timing and temperature. To summarise; years with higher diatom abundance had higher zooplankton biomass (at least until 2013), and in cold years the abundance of copepods was shifted later in the year.

3.3. Community composition

83 phytoplankton taxa were recorded during the time series and 89 mesozooplankton taxa (eggs and microplankton groups such as tintinnids and foraminifera were excluded). Table 2 shows the most abundant 30 taxa for phytoplankton and zooplankton in spring and in late summer. While many taxa are common to both seasons, their relative abundance does change (their position in the table) and contributes to
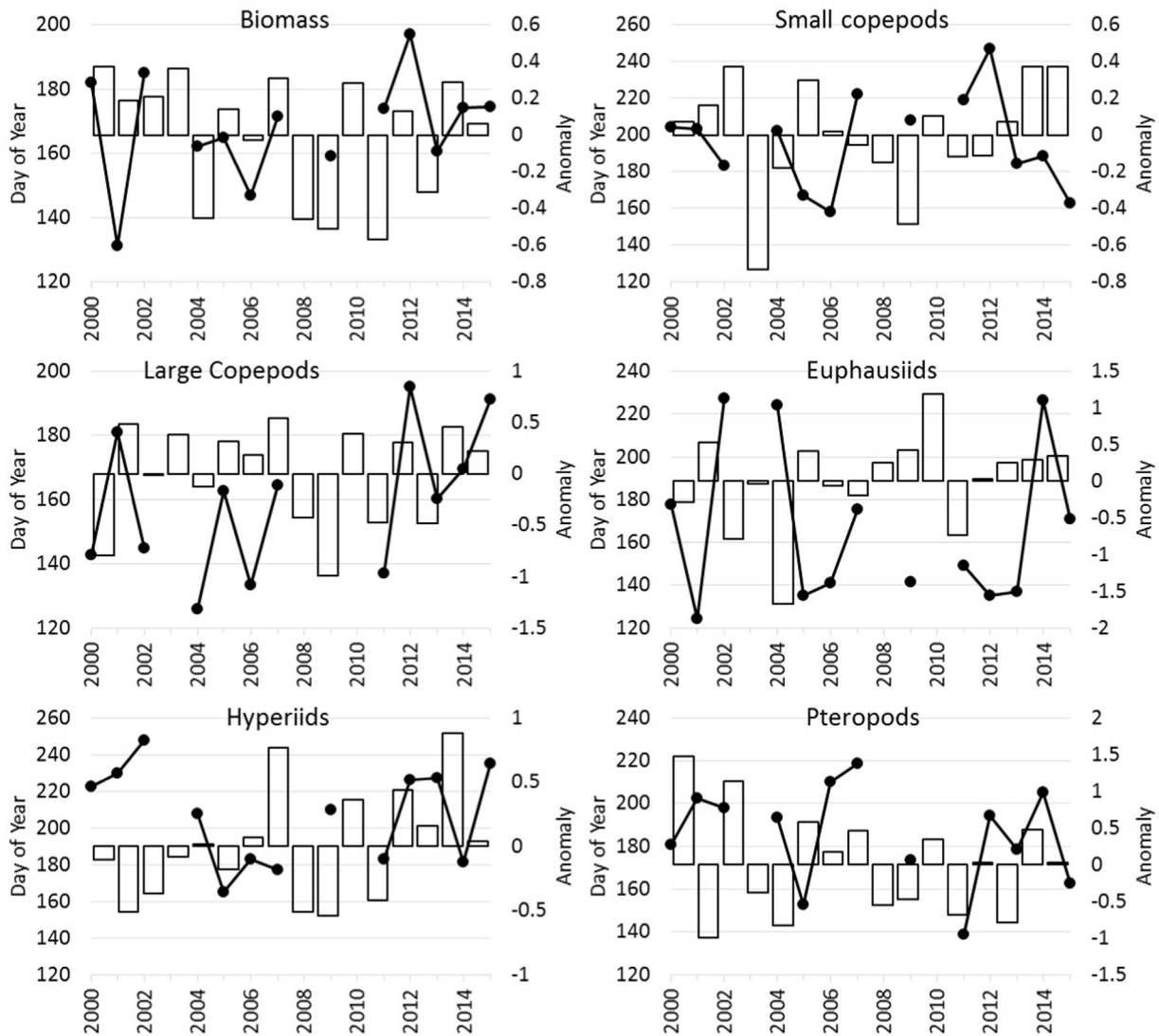
Fig. 6. Annual anomalies of zooplankton groups (bars) and seasonal timing (lines with dots). Top left panel shows total mesozooplankton biomass (estimated from taxonomic abundance data, see methods). Other five panels show abundance anomalies for groups as indicated; large copepods (length > 2 mm), small copepods (length < 2 mm), euphausiids, hyperiids, and pteropods.

the community differences seen between seasons. Some taxa are only abundant in one season; for example, dinoflagellates of the genus *Ceratium* are more common in late summer and the large *Neocalanus* copepods are typically only found in surface waters in spring. The MDS plots (Figs. 7 and 8) are 2 dimensional representations of the similarity of the spring or late summer/autumn communities between years (using all the taxa), so that years with the most similar communities in each treatment plot closest together. Stress values were moderately low, being between 0.12 and 0.17 for all analyses indicating that a two dimensional representation was appropriate.

3.3.1. Phytoplankton

The MDS analyses in Fig. 7 show no strong division between the two time periods of sampling, first adjacent to PWS (2000–2003) and then Cook Inlet from 2004 onwards (e.g., in the spring analysis 2002 plots closer to 2008 and 2013 than it does to 2000 or 2001 and the autumn analysis is similarly mixed). This suggests a similar phytoplankton community across the wider southern Alaska shelf (at least as the CPR sees it), likely a result of the distribution of plankton along the shelf by the Alaska Coastal Current.

In the spring analysis there is one main cluster with 3 years somewhat more distant and therefore dis-similar to other years; 2005, 2007,

and 2015. The x-axis has little variability along it and the greater variability on the y-axis is likely related to temperature, with most of the warmer years plotting negatively on this axis. The exception is 2005, however, if this year is removed the relationship between temperature and the y-axis is significantly correlated ($r^2 = 0.40$, $p < 0.01$). 2015 is quite distinct; as well as having generally low numbers of diatoms overall (Fig. 4), there were several taxa found for the first time in the region in spring 2015 (e.g. *Dactyliosolen fragilissimus* and *Guinardia striata*) and some taxa commonly found in late summer but which occurred in spring 2015 for the first time (*Bacteriastrum* spp, *Ceratium tripos*).

In the late summer/autumn analysis 2010 and 2008 plot distantly from other years and account for the variability along the x-axis. The y-axis has years with higher numbers of dinoflagellates (such as *Ceratium* spp.) plotting positively, and this axis is also positively correlated with temperature ($p = 0.07$) and potential energy ($p = 0.06$). Dinoflagellates prefer warm, well-stratified conditions.

3.3.2. Zooplankton

The PWS shelf samples from 2000 to 2003 do not cluster separately from the 2004–2015 Cook Inlet shelf samples in the zooplankton analyses either (Fig. 8). In the spring analysis the years 2000 and 2009

Table 2
The 30 most abundant phytoplankton and zooplankton taxa occurring in each season.

Phytoplankton, Spring	Phytoplankton, Late Summer	Zooplankton, Spring	Zooplankton, Late Summer
Thalassiosira spp.	Thalassionema nitzschioides	Pseudocalanus spp. C6	Pseudocalanus spp. C6
Chaetoceros spp. (Hyalochaetes)	Bacteriastrum spp.	Acartia longiremis	Acartia longiremis
Chaetoceros spp. (Phaeoceros)	Thalassiosira spp.	Calanus spp. C1-4	Echinoderm larvae
Corethron hystrix	Silicoflagellatae	cirrpede larva	Calanus spp. C1-4
Thalassionema nitzschioides	Chaetoceros spp. (Hyalochaetes)	Neocalanus plumchrus C5	Oithona spp.
Silicoflagellatae	Chaetoceros spp. (Phaeoceros)	Echinoderm larvae	Acartia spp.
Neodenticula seminae	Pseudo-nitzschia seriata	Limacina helicina	Appendicularia
Unidentified Coscinodiscus spp.	Thalassiothrix longissima	Oithona spp.	Limacina helicina
Odontella aurita	Ceratium fusus	Euphausiacea calyptopis	Centropages abdominalis
Thalassiothrix longissima	Skeletonema costatum	Acartia spp.	Calanus pacificus C5-6
Rhizosolenia hebetata semispina	Rhizosolenia hebetata semispina	Neocalanus plumchrus/flemingeri C4	Euphausiacea calyptopis
Skeletonema costatum	Pseudo-nitzschia delicatissima complex	Appendicularia	Podon spp.
Pseudo-nitzschia delicatissima complex	Rhizosolenia setigera	Neocalanus plumchrus/flemingeri C2	Cirripede larva
Coccolithaceae	Detonula confervacea	Neocalanus flemingeri C5	Tortanus discaudatus
Rhizosolenia styliformis	Ceratium lineatum	Cirripede nauplii	Clausocalanus spp.
Hyalochaete resting spore	Ditylum brightwellii	Euphausiacea	Calanus marshallae C5-6
Proboscia alata	Ceratium pentagonum	Calanus marshallae C5-6	Cyphonautes larva
Dinoflagellate cysts	Ceratium longipes	Clausocalanus spp.	Acartia danae
Ceratium pentagonum	Ceratium tripos	Decapoda larvae	Decapoda larvae
Pseudo-nitzschia seriata	Coscinodiscus spp.	Chaetognatha juveniles	Paracalanus spp. C6
Protoperidinium spp.	Coccolithaceae	Centropages abdominalis	Metridia pacifica C5-6
Stephanopyxis spp.	Biddulphia longicruris	Metridia spp. C1-4	Harpacticoida Total
Guinardia striata	Neodenticula seminae	Neocalanus cristatus C5-6	Chaetognatha juvenile
Cylindrotheca closterium	Pterosperma spp.	Neocalanus plumchrus/flemingeri C3	Euphausiacea
Ditylum brightwellii	Coscinodiscus concinnus	Cyphonautes larva	Neocalanus plumchrus/flemingeri C2
Detonula confervacea	Proboscia alata	Lamellibranch larvae	Hyperiidea
Unidentified Nitzschia spp.	Hyalochaete resting spore	Eurytemora pacifica	Evadne spp.
Ceratium furca	Ceratium horridum	Hyperiidea	Lamellibranch larvae
Ceratium horridum	Cylindrotheca closterium	Metridia pacifica C5-6	Ctenocalanus spp.
Paralia sulcata	Dinoflagellate cysts	Paracalanus spp. C6	Chaetognatha Adult
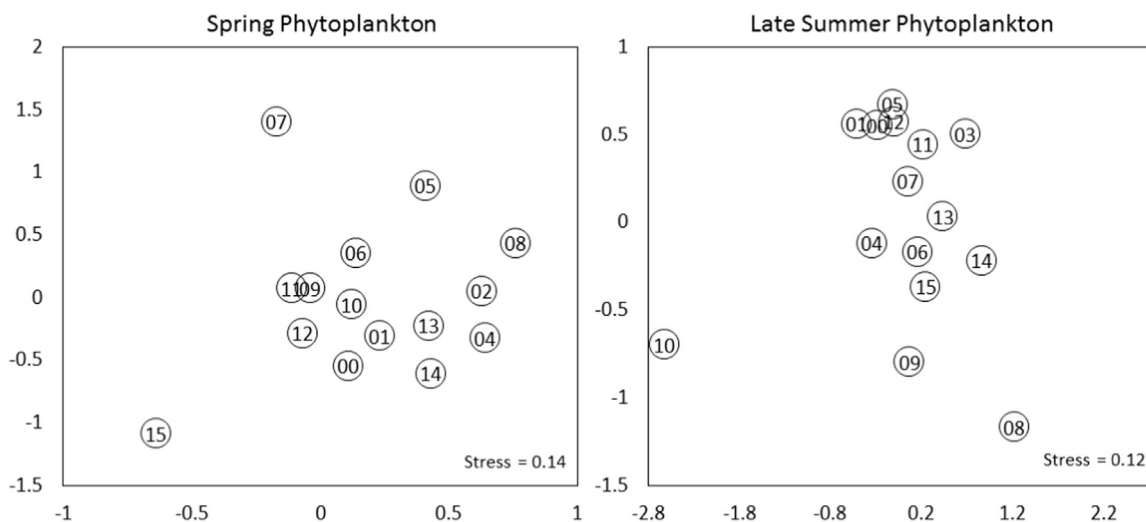
Fig. 7. Non-Metric Multidimensional Scaling analysis results of transformed spring (left, April to June) and late summer (right, August and September) phytoplankton taxonomic abundance data. The year is given in the centre of each point. Stress values for each ordination are given in the lower right.

appear to be different from other years, and different from each other. Examination of the taxa showed that several copepod taxa were absent or in low abundance in 2000 and there were high numbers of pteropods in this year (also evident from the anomaly plots in Fig. 6 where copepods were low in numbers and pteropods were high). The year 2009 contained some occurrences of rarer taxa such as *Paraeuchaeta* spp., sergestids and higher numbers of appendicularians. These taxa were present in some other years, but their combined effects influenced the overall difference in 2009 community composition. There were no strong relationships between the axes and physical variables. The y-axis of the spring plot is likely related to the PDO/temperature with PDO positive, warm years mostly positive on this axis. 2008 is, however, in the centre and not as negative as might be expected if this relationship

was a significant driver.

The late summer analysis has several years near the lower half of the plot that are dis-similar to the main cluster with 2003 standing out as particularly distinct. Many taxa were absent in this year and two copepod taxa, *Epilabidocera* spp. and *Centropages abdominalis* were relatively abundant. The y-axis of this plot relates strongly to the abundance of diatoms. Years with a positive diatom anomaly plot negatively on the y-axis while years with low numbers of diatoms are near the top ($r^2 = 0.44$, $p < 0.01$) suggesting a relationship between phytoplankton abundance and zooplankton community structure.

3.3.3. Copepod community size

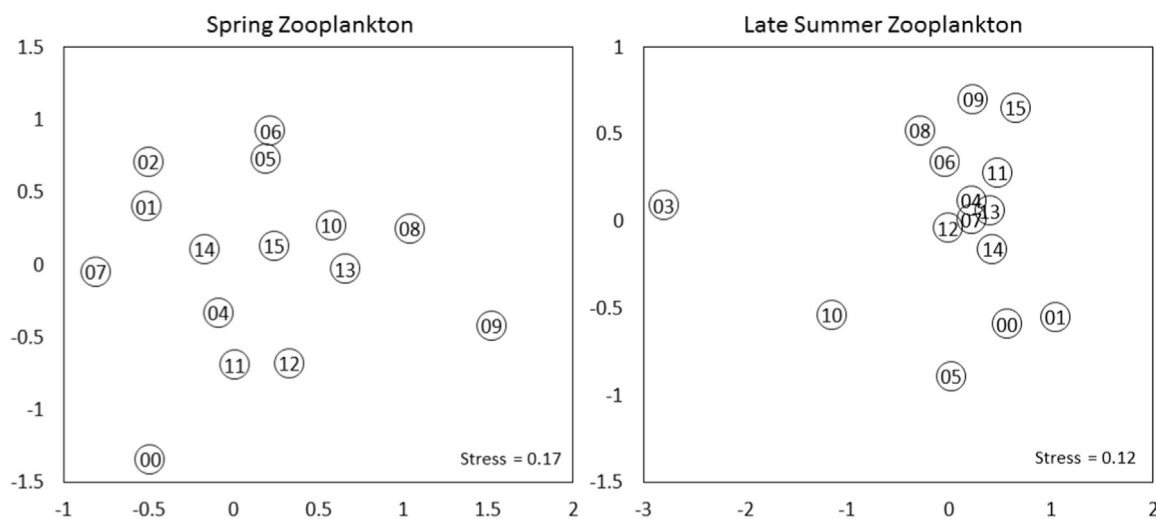A total of 43 copepod taxa were recorded, ranging from individual

Fig. 8. Non-Metric Multidimensional Scaling analysis results of transformed spring (left, April to June) and late summer (right, August and September) zooplankton taxonomic abundance data. The year is given in the centre of each point. Stress values for each ordination are given in the lower right.
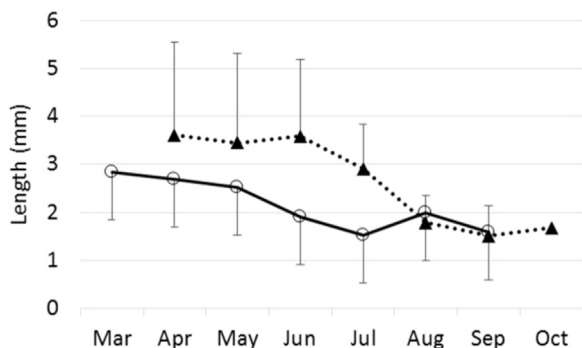

Fig. 9. Monthly mean copepod length (mean Copepod Community Size, see methods section for derivation) for the 5 warmest years (solid line with circles) and the 5 coldest years (dashed line with triangles). Error bars show standard deviation (in one direction only to avoid clutter).

stages in the case of the dominant species *Neocalanus plumchrus* (stages C2 to C6 were separately counted, though adults were rare) to genus level for those species more difficult to distinguish such as *Oithona* spp. The dominant taxa are shown in Table 2. The seasonal cycle of copepod community size, or the mean length of copepods in the community as represented by adult female length, (CCS) is shown in Fig. 9 and reveals the expected pattern where large copepods are more prevalent earlier in spring and, as these species descend to diapause in summer, the community becomes dominated by smaller species reducing the CCS, as reported in Coyle and Pinchuk (2003). The influence of temperature on the copepod community is clear, however, with the group of 5 warmest years having significantly smaller mean CCS in all spring and early summer months than the group of 5 coldest years (*t*-test, *p* < 0.05 for April and May, *p* < 0.0001 for June and July). Smaller species are both more numerous in warm than in cold years and have an earlier seasonal cycle, both factors contributing to a lower CCS in warm years. In August and September there was no significant difference in CCS between groups of years since even in cold years large *Neocalanus* copepods have almost all entered diapause by this time and the community is always dominated by smaller species such as *Acartia, Pseudocalanus* and *Paracalanus* spp.

4. Discussion

Our analyses have treated the shelf as one water body, which is an over-simplification since influences of the various current systems which run along the shelf will likely be different on the inner versus the outer shelf. The large scale resolution of CPR sampling (each sample covers 18.5 km) is some mitigation for this approach. Where whole-shelf temperature data from the CPR logger are available (Fig. 2, Section 3.1) they show the same broad inter-annual patterns as the GAK1 time series but this is only part of the story. Horizontal temperature gradients on the Gulf of Alaska shelf are weak compared to salinity gradients but there are, however, cross-shelf gradients in stratification. In spring, the inner half of the shelf stratifies primarily due to salinity and is thus affected by the magnitude and/or timing of winter and spring runoff (Janout et al., 2010). In contrast, the onset of springtime stratification over the outer half of the shelf is controlled by vertical temperature gradients. However, anomalously weak downwelling (or upwelling-favourable) winds can spread low-salinity waters over the outer shelf and thereby affect the stratification here meaning salinity variability has a strong influence on water column structure across the entire shelf (Weingartner et al., 2002). We may therefore expect climate forcing which influences the timing and intensity of freshwater run-off from the surrounding watersheds to have a large influence on the plankton. Temperature variability will also impact lower trophic levels directly in a number of ways; via basic metabolic processes with temperature-dependent rates and for at least some species the timing of life history events is related to ambient temperature (e.g. Batten et al., 2003c). We would therefore expect physical processes which create variability in either, or both, freshwater and heat content of the Alaskan Shelf waters to lead to variability in the plankton communities there.

Although the CPR was not designed as a phytoplankton sampler, and the mesh size is larger than many phytoplankton cells, there are nonetheless valuable insights into phytoplankton variability that can be gained from CPR data, because it is an internally consistent sampler and does retain a representative proportion of even quite small cells (especially if chain-forming). Fig. 3, Section 3.2.1 demonstrates that seasonal cycles derived from the CPR data closely replicate those seen from satellites for the same area, confirming that useful information can be gained. Through the first 14 years of the time series of CPR sampling on the Alaskan Shelf we have found that warm years had generally higher abundances of the larger cells retained by the CPR, particularly of diatoms (Fig. 4). The diatom anomaly time series has some similarity to a chlorophyll-*a* anomaly time series derived from satellite measurements for a wider area of the coastal Gulf of Alaska (Waite and Mueter, 2013). Their time series showed positive anomalies from 1998 to 2002, negative anomalies from 2003 to 2005, close to average for 2006–2010, and strongly negative in 2011. The CPR diatom anomalies were high in the early years also, suggesting a widespread event, and the decline in

the middle years was probably not related to the change in time series location since the Waite and Mueter study showed a similar decline in chlorophyll-*a* at this time. The strongly negative anomaly in 2011 was common to both studies. Causes of this low productivity year are still being explored, however, the CPR zooplankton data show that the effects passed up the food chain from the phytoplankton; zooplankton biomass had the lowest anomaly of the time series to date in 2011 (Fig. 6). Interestingly, the community composition analyses did not identify 2011 as an anomalous year (Figs. 7 and 8). In terms of the type of taxa present and their relative abundance, 2011 was quite similar to several other years.

Diatom spring timing revealed an influence of water column conditions (Fig. 5). We might expect temperature to have a direct effect on diatom timing but this was not apparent, instead it was the degree of water column stability in May that provided the influence with a less stable water column (particularly a deeper MLD and to a lesser extent the lower potential energy) having a later spring peak in diatoms. There was also a significant correlation with the NPGO index, which is known to explain salinity variability further south in the California Current system (Di Lorenzo et al., 2008). The NPGO reflects both regional and basin scale variations in wind-driven circulation and advection processes. The relationships between the diatom timing and MLD and NPGO emphasises that phytoplankton processes are very much dependent on the physical oceanographic conditions.

Hard-shelled dinoflagellates are numerically much less important than the diatoms, typically having an abundance one tenth that of the diatoms in the CPR data, so the decline over time seen in Fig. 4 is not likely to have had much influence on total phytoplankton biomass. It has, however, contributed to the changing phytoplankton community composition shown in Fig. 7 by influencing the late summer composition, when dinoflagellates are typically most abundant. The NMDS analysis also showed an influence of the spring stratification strength (potential energy, shown in Fig. 2.) on summer phytoplankton composition. While stratification data from summer would be desirable to examine this further, it is feasible that the water column stability measured in late spring (May) would influence the community structure in the late summer, especially the numbers and types of dinoflagellates that prefer well-stratified waters.

Total mesozooplankton biomass was strongly positively correlated with diatom abundance for the years 2000–2013. The CPR data up to 2013 support the hypothesis that the physical environment of the Gulf of Alaska shelf (temperature and water column stability) influences the phytoplankton (diatom abundance and timing, dinoflagellate abundance), which in turn controls the quantity of mesozooplankton. However, these relationships were not apparent in the warm years of 2014 and 2015 when diatoms were unexpectedly low, in what has been termed a "marine heatwave" (DiLorenzo and Mantua, 2016) influenced first by the anomaly known as the Blob (Bond et al., 2015) and then an El Niño in 2015. These two years had the highest numbers of small copepods recorded in the time series which also were biased earlier in the year than average (Fig. 6). It is possible that the data for these two years show top-down control of the large diatoms by copepod grazing pressure, which was not seen in other warm years with high diatoms and high zooplankton abundance/biomass such as 2005. It is unlikely that the higher temperatures caused a non-linear response of lower productivity in the diatoms since these species also occur further south where such temperatures are normal. An alternative explanation is that the unusual conditions caused an unfavourable nutrient regime which reduced the productivity of large diatoms. The taxa recorded by the CPR in spring 2014 and 2015 did show a bias towards diatoms with longer, narrow cells (e.g. *Proboscia* spp., *Thalassiothrix* spp. and pennate species). Fig. 10 shows that only 2004 had a similarly high proportion of such cells and the spring community composition analyses also show 2004 and 2014 as very similar. Cells with this narrow morphology have a high surface area to volume ratio which would facilitate the take-up of nutrients; studies have shown that smaller cells which also have a
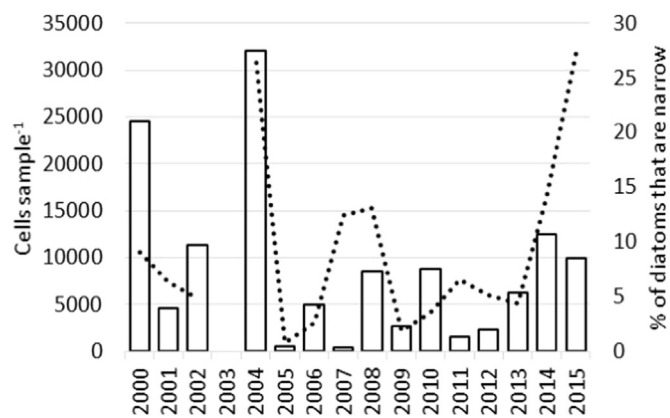

Fig. 10. Bars show the number of narrow, long diatom cells in spring of each year (April–June) while the dashed line shows the proportion of the total diatom community that they represent.

higher SA:Vol take up nutrients faster (Friebele et al., 1978; Geider et al., 1986). If nutrients were scarce they would have an advantage over the rounder cell types. However, the stratification indices shown in Fig. 2 do not suggest that 2014 and 2015 were especially stratified which might have limited the nutrients introduced by mixing. In 2015 there was an even higher proportion of these narrow cells, with low diatoms overall and high numbers of copepods still. The years 2014 and 2015 were also the only years of the time series when no coccolithophores were recorded in the samples, so other as yet unknown factors that influence phytoplankton community structure were also in play. It is also clear that the high numbers of copepods in these years must have been eating something, if not the large diatoms then some part of the plankton community not well resolved by the CPR.

Copepod seasonal timing is dependent on temperature since copepods are poikilothermic and their metabolic processes, including development rate, are faster in warm conditions (see Batten et al., 2003c; Mackas et al., 2007). The index of season mid-point calculated here ranged from day 126 to day 200 for large copepods, and day 163 to day 247 for small copepods. This is a considerable amount of variability – over 2 months in each case, and could potentially impact larger predators that time their reproduction or migration to take advantage of a peak in their prey. Zooplankton community composition was also likely influenced by temperature (Fig. 8 and Section 3.3.2). These changes were not as dramatic as a replacement of many species by others, rather a change in relative abundances with temporary occurrences of some rare species (*e.g.*, the copepod *Acartia danae*, usually found below 40°N but found in the CPR samples from the Alaskan shelf in the warm years 2005 and 2015). CPR data from the oceanic NE Pacific have noted the northwards extension of warm water species to the GOA in the warmest years of the last decade (Batten and Walne, 2011) and Hopcroft et al. (2007) report a seasonal ingress of southern species along the Seward Line also in the warm year 2005. As well as warm water species occurring, there is also a shift towards a smaller mean size of copepod (Fig. 9 and Section 3.3.3) through increased productivity of smaller species (which have multiple generations in one year) and an earlier increase in numbers. If smaller and/or warm water species contribute a significant amount to the zooplankton populations, they could present a dietary challenge to zooplankton predators assuming their nutritional quality varies from the more typical subarctic diet.

In summary, we have documented interannual variability in concentration and composition of the plankton community of the region over a 16 year time period. At least in part and suggested by correlative relationships, this variability can be attributed to changes in the physical environment, particularly temperature and its direct effects on metabolic processes as well as indirect effects on water column stability. The study ends with two anomalous years (2014 and 2015) for which previous relationships between temperature, diatom abundance

and small copepod abundance under warm conditions do not hold. The unusual warmth also continued into 2016 and impacts on the plankton communities from such sustained anomalous conditions remains unknown. The CPR continues to sample the Alaskan Shelf and given the rapidly changing climate the importance of regular, consistent sampling cannot be over-emphasised.

Acknowledgements

References

Batten, S.D., Walne, A.W., 2011. Variability in northwards extension of warm water copepods in the NE Pacific. J. Plankton Res. 33, 1643–1653.

Batten, S.D., Clarke, R.A., Flinkman, J., Hays, G.C., John, E.H., John, A.W.G., Jonas, T.J., Lindley, J.A., Stevens, D.P., Walne, A.W., 2003a. CPR sampling – the technical background, materials and methods, consistency and comparability. Prog. Oceanogr. 58, 193–215.

Batten, S.D., Walne, A.W., Edwards, M., Groom, S.B., 2003b. Phytoplankton biomass from Continuous Plankton Recorder data: an assessment of the phytoplankton colour index. J. Plankton Res. 25, 697–702.

Batten, S.D., Welch, D.W., Jonas, T., 2003c. Latitudinal differences in the duration of development of *Neocalanus plumchrus* copepodites. Fish. Oceanogr. 12 (3), 201–208.

Bond, N.A., Cronin, M.F., Freeland, H., Mantua, N., 2015. Causes and impacts of the 2014 warm anomaly in the NE Pacific. Geophys. Res. Lett. 42, 3414–3420. http://dx.doi.org/10.1002/2015GL063306.

Chihara, M., Murano, M. (Eds.), 1997. An Illustrated Guide to Marine Plankton in Japan. Tokai University Press, Tokyo, pp. 1574 (ISBN 4486012895).

Cooney, R.T., Coyle, K.O., Stockmar, E., Stark, C., 2001. Seasonality in surface-layer net zooplankton communities in Prince William Sound, Alaska. Fish. Oceanogr. 10, 97–109.

Coyle, K.O., Pinchuk, A.I., 2003. Annual cycle of zooplankton abundance, biomass and production on the northern Gulf of Alaska shelf, October 1997 through October 2000. Fish. Oceanogr. 12, 327–338.

DiLorenzo, E., Mantua, N., 2016. Multi-year persistence of the 2014/15 North Pacific marine heatwave. Nat. Clim. Change. http://dx.doi.org/10.1038/nclimate3082.

Di Lorenzo, E., Schneider, N., Cobb, K.M., Chhak, K., Franks, P.J.S., Miller, A.J., McWilliams, J.C., Bograd, S.J., Arango, H., Curchister, E., Powell, T.M., Rivere, P., 2008. North Pacific Gyre Oscillation links ocean climate and ecosystem change. Geophys. Res. Lett. 35, L08607. http://dx.doi.org/10.1029/2007GL032838.

Exxon Valdez Oil Spill Trustee Council, 2010. Exxon Valdez Oil Spill Restoration Plan: 2010 Update of Injured Resources and Services. EVOS Trustee Council, Anchorage, Alaska, pp. 48. (Available at). ⟨http://www.evostc.state.ak.us/Universal/Documents/Publications/2010IRSUpdate.pdf⟩.

Feldman, G.C., McClain, C.R., 2012. In: Kuring, N., Bailey, S.W. (Eds.), Ocean Color Web, MODIS Reprocessing R2009. NASA Goddard Space Flight Center. ⟨http://oceancolor.gsfc.nasa.gov⟩.

Francis, R.C., Hare, S.R., 1994. Decadal-scale regime shifts in the large marine ecosystems of the Northeast Pacific: a case for historical science. Fish. Oceanogr. 3, 279–291.

Friebele, E.S., Correll, D.L., Faust, M.A., 1978. Relationship between phytoplankton cell size and the rate of orthophosphate uptake: *in situ* observations of an estuarine population. Mar. Biol. 45, 39–52.

Geider, R.J., Platt, T., Raven, J.A., 1986. Size dependence of growth and photosynthesis in diatoms: a synthesis. Mar. Ecol. Prog. Ser. 30, 93–104.

Grieve, W., Prinage, S., Zidowitz, H., Nast, J., Reiners, F., 2005. On the phenology of North Sea ichthyoplankton. ICES J. Mar. Sci. 62, 1216–1223.

Hopcroft, R., Coyle, K., Weingartner, T., Whitledge, T., 2007. Gulf of Alaska Long-term Observations: the Seward Line. Final report to the North Pacific Research Board, Dec 2007.

IOCCG, 2000. Remote Sensing of Ocean Colour in Coastal, and Other Optically-Complex Waters Rep. No. 3 IOCCG, Dartmouth, Canada.

Janout, M.A., Weingartner, T.J., Royer, T.C., Danielson, S.L., 2010. On the nature of winter cooling and the recent temperature shift on the northern Gulf of Alaska shelf. J. Geophys. Res.: Oceans 115, 2156–2202.

Ladd, C., Kachel, N.B., Mordy, C.W., Stabeno, P.J., 2005. Observations from a Yakutat eddy in the northern Gulf of Alaska. J. Geophys. Res.: Oceans 110, C03003 (doi: 03010.01029/02004JC002710).

Mackas, D.L., Batten, S.D., Trudel, M., 2007. Effects on zooplankton of a warming ocean: recent evidence from the Northeast Pacific. Prog. Oceanogr. 75, 223–252.

Mantua, N.J., Hare, S.R., Zhang, Y., Wallace, J.M., Francis, R.C., 1997. A Pacific decadal climate oscillation with impacts on salmon. Bull. Am. Meteorol. Soc. 78, 1069–1079.

Mueter, F.J., Broms, C., Drinkwater, K.F., Friedland, K.D., Hare, J.A., Hunt, G.L., Webjorn, M., Taylor, M., 2009. Ecosystem responses to recent oceanographic variability in high-latitude Nortehrn hemisphere ecosystems. Prog. Oceanogr. 81, 93–110.

Okkonen, S.R., Weingartner, T.J., Danielson, S.L., Musgrave, D.L., 2003. Satellite and hydrographic observations of eddy-induced shelf-slope exchange in the northwestern Gulf of Alaska. J. Geophys. Res. 108 (C2), 3033. http://dx.doi.org/10.1029/2002JC001342.

O'Reilly, J.E. (Ed.), 2000. SeaWiFS Postlaunch Calibration and Validation Analyses, Part 3. NASA Goddard Space Flight Centre, Greenbelt, Maryland.

Raitsos, D.E., Walne, A., Lavender, S.J., Licandro, P., Reid, P.C., Edwards, M., 2013. A 60-year ocean colour data set from the continuous plankton recorder. J. Plankton Res. 35 (1), 158–164.

Razouls, C., de Bovée, F., Kouwenberg, J., Desreumaux, N. 2005–2012. Diversity and Geographic Distribution of Marine Planktonic Copepods. Available at ⟨http://copepodes.obs-banyuls.fr/en⟩.

Richardson, A.J., Walne, A.W., John, A.W.G.J., Jonas, T.D., Lindley, J.A., Sims, D.W., Stevens, D., Witt, M., 2006. Using continuous plankton recorder data. Prog. Oceanogr. 68, 27–74.

Royer, T.C., 1979. On the effect of precipitation and runoff on coastal circulation in the Gulf of Alaska. J. Phys. Oceanogr. 9, 555–563.

Simpson, J.H., Hughes, D.H., Morris, N.C.G., 1977. In: Angel, M.V. (Ed.), The Relation of the Seasonal Stratification to Tidal Mixing on the Continental Shelf. A Voyage of Discovery. Pergamon, London, pp. 327–340 George Deacon 70th anniversary volume.

Stabeno, P.J., Bond, N.A., Hermann, A.J., Kachel, N.B., Mordy, C.W., Overland, J.E., 2004. Meteorology and oceanography of the Northern Gulf of Alaska. Cont. Shelf Res. 24, 859–897.

Waite, J.N., Mueter, F.J., 2013. Spatial and temporal variability of chlorophyll-a concentrations in the coastal Gulf of Alaska, 1998–2011, using cloud-free reconstructions of SeaWiFS and MODIS-Aqua data. Prog. Oceanogr. 116, 179–192.

Weingartner, T.J., Danielson, S.L., Royer, T.C., 2005. Freshwater variability and predictability in the Alaska coastal current. Deep Sea Res. Part II: Top. Stud. Oceanogr. 52, 169–191.

Weingartner, T.J., Coyle, K.O., Finney, B., Hopcroft, R., Whitledge, T., Brodeur, R.D., Dagg, M., Farley, E., Haidvogel, D., Haldorson, L., Herman, A., Hinckley, S., Napp, J.M., Stabeno, P.J., Kline, T., Lee, C., Lessard, E., Royer, T., Strom, S., 2002. The Northeast Pacific GLOBEC program: coastal Gulf of Alaska. Oceanography 15, 48–63.